Real Space Green's Function Approach to Vibrational Dynamics of a Vicsek Fractal

C. S. Jayanthi,[1] S. Y. Wu,[1] and J. Cocks[2]
[1]*Department of Physics, University of Louisville, Louisville, Kentucky 40292*
[2]*Computing and Telecommunications, University of Louisville, Louisville, Kentucky 40292*
(Received 3 February 1992)

A new method to determine eigenvectors based on a real space Green's function is reported. This method is particularly useful for determining the eigenvectors corresponding to degenerate states. Using this approach, the lowest persistent degenerate mode exhibited by the third-stage Vicsek fractal has been examined and has been shown to be an edge-confined, superlocalized vibrational mode.

PACS numbers: 63.20.Pw, 63.50.+x, 64.60.Ak

Eigenvalue problems are ubiquitous in physics. However, to our knowledge there is no unique way to determine eigenvectors corresponding to degenerate eigenvalues. In using traditional approaches, it is assumed at the outset that any linear combination of eigenvectors is also a valid eigenvector for a degenerate eigenvalue and then a Gram-Schmidt scheme is used to find a set of orthogonal eigenvectors that spans the degenerate subspace [1]. In such an approach, if arbitrary linear combinations are chosen, the resultant eigenvectors may not possess the actual symmetry of the physical system at hand. In order to get the correct symmetry from such an approach, often, a prior insight into the problem is necessary.

In this Letter it is shown that eigenvectors possessing the correct local symmetry can be obtained from a real space Green's function. The unique feature of this approach is demonstrated by studying the dynamics of a Vicsek fractal. In particular, we focus our investigation on the persistent degenerate modes exhibited by the eigenvalue spectrum of the Vicsek fractal. The eigenvectors corresponding to these modes are shown to be edge-confined, superlocalized vibrational states.

Recently, a confined vibrational mode similar to the one exhibited by the Vicsek fractal has been observed on a fractal drum [2]. The framework of this drum has been designed to resemble the third-generation quadratic Koch curve. The common feature of the quadratic Koch curve and the Vicsek fractal is that both of them possess four equivalent branches. According to Sapoval, Gobron, and Margolina [2], the most puzzling feature of the experimental observation is that the vibrational mode is confined to one of the branches in spite of the presence of the four equivalent regions. To explain this observation, Sapoval, Gobron, and Margolina calculated the first four lowest excited modes of the fractal drum and found that a linear superposition of these modes can lead to a confined mode although none of these modes was localized individually. However, the confined mode constructed this way would not remain confined in a specific region of space in the time-dependent picture. Therefore, the above explanation may not fully account for the experimental observation. Using our approach to analyze the dynamics of the Vicsek fractal, a low-lying, edge-confined vibrational state emerges quite naturally from a persistent degenerate mode. To our knowledge, this is the first evidence of an edge-confined mode in a Vicsek fractal, although the eigenvalue spectrum of this fractal has been studied earlier [3]. Also, such an edge-confined mode has not been reported for the widely studied Sierpinski gasket which is known to exhibit other types of localized modes [4].

We first derive the formula relating the eigenvector to the real space Green's function. An eigenvalue problem $H|v_i\rangle = z_i|v_i\rangle$ can usually be written in terms of the Green's function $R=(z-H)^{-1}$ such that

$$\sum_m R_{lm}^{-1}(z)u_m = 0\,, \tag{1}$$

where $u_m = \langle m|v_i\rangle$ defines the eigenvector in a complete set of orthonormal basis $|m\rangle$. If a set of site-dependent basis vectors is chosen for $|m\rangle$, then the Green's function expressed in terms of this basis set is referred to as a real space Green's function. If we now make use of the identity

$$\sum_m R_{lm}^{-1}(z+i\varepsilon)R_{mk}(z+i\varepsilon) = \delta_{lk} \tag{2}$$

and take the imaginary part of Eq. (2), we obtain

$$\sum_m R_{lm}^{-1}(z)\mathrm{Im}R_{mk}(z+i\varepsilon) + \varepsilon \mathrm{Re}R_{lk}(z+i\varepsilon) = 0\,, \tag{3}$$

where we have used the fact that $R_{lm}^{-1}(z+i\varepsilon) = R_{lm}^{-1}(z) + i\varepsilon\delta_{lm}$. A comparison of Eqs. (3) and (1) indicates that, as $\varepsilon \to 0$, $\mathrm{Im}R_{mk} \sim u_m$. This result indicates that the kth column of $\mathrm{Im}R(z_i)$ yields the eigenvector corresponding to the eigenvalue z_i. If the eigenvector is scaled using the diagonal element, namely, $\mathrm{Im}R_{kk}$, one can write the corresponding eigenvector as

$$|z\rangle_k = \sum_m \frac{\mathrm{Im}_{\varepsilon\to 0}R_{mk}(z+i\varepsilon)}{\mathrm{Im}_{\varepsilon\to 0}R_{kk}(z+i\varepsilon)}|m\rangle\,. \tag{4}$$

In using this method to determine the eigenvector, it is found that, for a nondegenerate eigenvalue, any one of the N columns of $\mathrm{Im}_{\varepsilon\to 0}R(z+i\varepsilon)$ corresponds to a valid eigenvector. This is because either all columns are identical or they differ from one another by a constant multiplicative factor. On the other hand, for a g-fold degenerate eigenvalue, there will be g independent column vectors among the N column vectors of $\mathrm{Im}_{\varepsilon\to 0}R(z+i\varepsilon)$. In ad-

dition, it should be noted that, in this case, each of the column vectors of ImR represents a possible eigenstate weighted by the amplitude of the eigenvector at the basis vector corresponding to the column in question. To see this, note that [5]

$$\mathrm{Im}R(z+i\varepsilon) = -\sum_{\mu} \frac{|\mu\rangle\langle\mu|\varepsilon}{(z-\mu)^2+\varepsilon^2}, \tag{5}$$

where $|\mu\rangle$ denotes the complete set of orthonormal eigenvectors of H. Substitution of Eq. (5) into Eq. (4) then shows that, for a g-fold degenerate eigenvalue λ,

$$|\lambda\rangle_k = \frac{1}{\sum_\lambda |\langle\lambda|k\rangle|^2} \sum_{\lambda} |\lambda\rangle\langle\lambda|k\rangle, \tag{6}$$

where the summation over λ in Eq. (6) runs through the g orthonormal, degenerate eigenvectors $|\lambda\rangle$. Therefore, we find that the kth column vector of ImR, namely, $|\lambda\rangle_k$, which is a linear combination of the g degenerate eigenvectors of λ, is a valid eigenvector. It is an eigenvector weighted by the amplitudes of $|\lambda\rangle$ on the basis vector $|k\rangle$ and if a local basis vector $|k\rangle$ is used to define the matrix H then the eigenvector obtained from this calculation would have the correct local information.

We have used the above method to analyze the vibrational states of the first three stages of a Vicsek fractal with a rigid boundary. We restrict ourselves to the third-generation Vicsek fractal because we would like to show the analogy between the dynamics of the Vicsek fractal and the available experimental results on the fractal drum [2]. The third-stage Vicsek fractal with its boundary atoms anchored is shown in Fig. 1. The transverse vibration of a Vicsek fractal can be described by a matrix in the representation of the local displacement vectors [6]. The matrix for the first-stage Vicsek gasket (as shown by the five-particle cluster at the center of Fig. 1) with its outer particles anchored to a rigid boundary can be expressed as

$$H_1 = \begin{pmatrix} 4\gamma/m & -\gamma/m & -\gamma/m & -\gamma/m & -\gamma/m \\ -\gamma/m & 2\gamma/m & 0 & 0 & 0 \\ -\gamma/m & 0 & 2\gamma/m & 0 & 0 \\ -\gamma/m & 0 & 0 & 2\gamma/m & 0 \\ -\gamma/m & 0 & 0 & 0 & 2\gamma/m \end{pmatrix}, \tag{7}$$

where γ is the force constant and m is the mass of the particle. The matrix for the subsequent stage can be built easily from the previous stage because of the self-similar nature of the fractal. For example, the matrix of the nth-stage fractal can be constructed from the $(n-1)$th-stage fractal as follows:

$$H_n = \begin{pmatrix} H_{n-1} & V & V & V & V \\ V^T & H_{n-1} & 0 & 0 & 0 \\ V^T & 0 & H_{n-1} & 0 & 0 \\ V^T & 0 & 0 & H_{n-1} & 0 \\ V^T & 0 & 0 & 0 & H_{n-1} \end{pmatrix}, \tag{8}$$

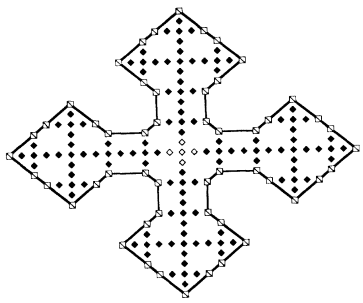

FIG. 1. The third-generation Vicsek fractal with its boundary atoms anchored. The anchoring locations are marked by the open symbols and the fractal boundary by the solid line. The first-stage fractal is shown by the five-particle cluster at the center ($\diamond$).

where V's are the matrices describing the interactions between the central cluster and the four outer clusters. The equivalence of the four outer clusters to the fractal of the previous stage, which is a reflection of the self-similar nature of the fractal, is clearly seen in Eq. (8).

The eigenvalue spectrum of the first three stages of the Vicsek fractal has been computed using Eqs. (7) and (8). The most interesting feature of the eigenvalue spectrum is that the degenerate modes of a given stage persist in all higher generations (Table I). For example, the threefold degenerate mode of the first generation, namely, $\omega^2 = 2.0$ (in the reduced unit of $\gamma/m = 1$) persists in the second generation as an eightfold degenerate mode and in the third generation as a 32-fold degenerate mode. The degree of degeneracy of the persistent mode in all higher generations can be predicted. For $n \geq 3$, it follows the pattern $D_n = 5D_{n-1} - 8$, where D_n is the degree of degeneracy of the persistent mode at the nth stage. In general, one can predict the pattern of evolution of the entire eigenvalue spectrum from a given stage to the next. This will be discussed elsewhere [7].

In what follows, we shall focus on the lowest persistent mode of the third-stage Vicsek gasket, namely, $\omega^2 = 0.563$. This mode first appears in the second stage as a threefold degenerate mode and it becomes an eightfold degenerate mode in the third stage. The eigenvectors corresponding to these modes were calculated using the

TABLE I. First few low-lying vibrational states of a Vicsek fractal.

First stage	Second stage	Third stage
0.76393 (1)	0.19817 (1)	0.16301 (1)
2.00000 (3)	0.56300 (3)	0.18968 (3)
5.23607 (1)	0.94735 (1)	0.20254 (1)
	1.28364 (3)	0.35887 (3)
	2.00000 (8)	0.44622 (1)
	2.29464 (1)	0.56300 (8)
	2.89418 (3)	0.60846 (3)
	⋮	⋮

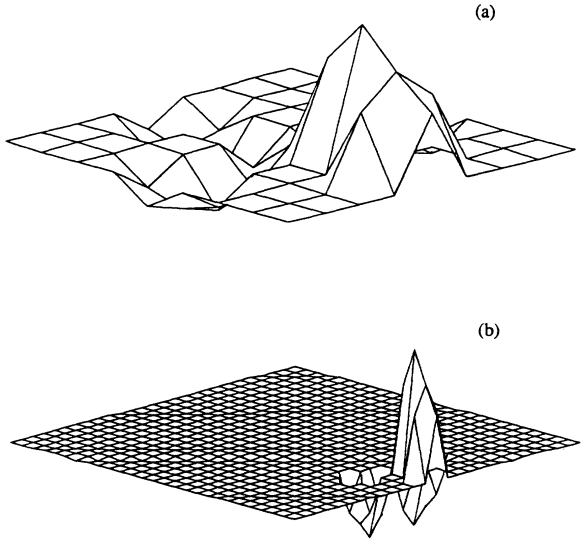

FIG. 2. One of the eigenvectors of the threefold degenerate mode ($\omega^2=0.56300$) of the second generation is shown in (a). (b) The same mode evolves into an edge-confined mode in the third stage.

real space Green's function [Eq. (4)]. Figure 2(a) shows one of the eigenvectors of the threefold degenerate mode and Fig. 2(b) shows how this mode becomes an edge-confined superlocalized mode in the third stage. A detailed analysis of the eigenvectors corresponding to the above modes is given below with a view to understand the nature of the mode and the pattern of evolution of the eigenvalue spectrum.

The eigenvector shown in Fig. 2(a) [denoted by $u_2^{\{3\}}(1)$, where the superscript refers to the degree of degeneracy, the subscript to the stage, and the number in parentheses to one of the eigenvectors] can be expressed as $\mathbf{u}_2^{\{3\}}(1)=\{0,\tilde{\mathbf{u}}_1(a),\tilde{\mathbf{u}}_1(b),\tilde{\mathbf{u}}_1(c),\tilde{\mathbf{u}}_1(d)\}$. Here the displacement of the central atom is zero [see Fig. 2(a)] and $\tilde{\mathbf{u}}_1$'s are the displacement vector fields associated with the four equivalent regions (a,b,c,d) surrounding the central atom where the equivalent regions under consideration have six particles, as shown in Fig. 3. Furthermore, it can be seen from Table II that $\tilde{\mathbf{u}}_1(a)=\tilde{\mathbf{u}}_1(b)=\tilde{\mathbf{u}}_1(c)=\mathbf{A}$

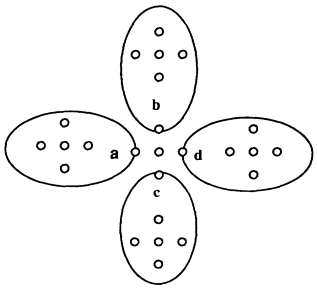

FIG. 3. Partitioning of the second-stage Vicsek fractal into four equivalent regions surrounding the central particle as used in the description of the eigenvector $\mathbf{u}_2^{\{3\}}(1)$.

TABLE II. One of the eigenvectors of the threefold degenerate mode $\omega^2=0.563$ of the second-stage fractal: $\mathbf{u}_2^{\{3\}}(1)=(0,\tilde{\mathbf{u}}_1(a),\tilde{\mathbf{u}}_1(b),\tilde{\mathbf{u}}_1(c),\tilde{\mathbf{u}}_1(d))$.

$\tilde{\mathbf{u}}_1(a)$	$\tilde{\mathbf{u}}_1(b)$	$\tilde{\mathbf{u}}_1(c)$	$\tilde{\mathbf{u}}_1(d)$
−0.232	−0.232	−0.232	0.696
−0.333	−0.333	−0.333	1.0
−0.247	−0.247	−0.247	0.741
−0.172	−0.172	−0.172	0.516
−0.172	−0.172	−0.172	0.516
−0.172	−0.172	−0.172	0.516

and $\tilde{\mathbf{u}}_1(d)=-3\mathbf{A}$ for the eigenvector in question. In addition, there are three other eigenvectors corresponding to this mode, namely, $\mathbf{u}_2^{\{3\}}(2)=\{0,\mathbf{A},-3\mathbf{A},\mathbf{A},\mathbf{A}\}$, $\mathbf{u}_2^{\{3\}}(3)=\{0,\mathbf{A},\mathbf{A},-3\mathbf{A},\mathbf{A}\}$, and $\mathbf{u}_2^{\{3\}}(4)=\{0,-3\mathbf{A},\mathbf{A},\mathbf{A},\mathbf{A}\}$. Therefore, $\sum_{i=1}^{4}\mathbf{u}_2^{\{3\}}(i)=0$. This indicates that there are only three independent eigenvectors. Clearly, this picture is consistent with the threefold degeneracy of the mode. In order for the threefold degenerate mode ($\omega_p^2=0.563$) of the second stage to persist in the third stage, a vibrational configuration similar to that of the second stage must exist in the third stage. For this to happen, $\omega=\omega_p$ must satisfy eigenvalue equations of the second stage and the third stage simultaneously. It can be realized only if the displacement vector field of all particles in the central (25-particle) cluster of the third stage becomes zero, decoupling the outer clusters from each other. This is a consequence of the self-similarity reflected by Eq. (8), indicating that the existence of the persistent mode is intimately linked to the self-similar nature of the fractal.

Next, consider the eigenvector shown in Fig. 2(b). This eigenvector can be represented by $\mathbf{u}_3^{\{8\}}(1)=\{\mathbf{0},\mathbf{0},\mathbf{0},\mathbf{0},\mathbf{u}_2(d)\}$, where $\mathbf{u}_2(d)$ is the displacement vector field of the second-stage cluster located in the region d of the third stage while the displacement fields of other clusters vanishes as represented by the boldface zeros. In particular, $\mathbf{u}_2(d)=\{0,\tilde{\mathbf{u}}_1(a),\tilde{\mathbf{u}}_1(b),\tilde{\mathbf{u}}_1(c),\tilde{\mathbf{u}}_1(d)\}$ with $\tilde{\mathbf{u}}_1(a)=\mathbf{0}$, $\tilde{\mathbf{u}}_1(b)=\tilde{\mathbf{u}}_1(c)=\mathbf{B}$, and $\tilde{\mathbf{u}}_1(d)=-2\mathbf{B}$, as can be seen from Table III. The edge-confined nature of the persistent mode is clearly seen from the structure of the eigenvector $\mathbf{u}_3^{\{8\}}(1)$. In addition, there are two other eigenvectors, $\mathbf{u}_2(2)=\{0,\mathbf{0},-2\mathbf{B},\mathbf{B},\mathbf{B}\}$, and $\mathbf{u}_2(3)=\{0,\mathbf{0},\mathbf{B},-2\mathbf{B},\mathbf{B}\}$

TABLE III. One of the eigenvectors of the eightfold degenerate mode $\omega^2=0.563$ of the third stage: $\mathbf{u}_3^{\{8\}}(1)=\{\mathbf{0},\mathbf{0},\mathbf{0},\mathbf{0},\mathbf{u}_2(d)\}$, $\mathbf{u}_2(d)=\{0,\tilde{\mathbf{u}}_1(a),\tilde{\mathbf{u}}_1(b),\tilde{\mathbf{u}}_1(c),\tilde{\mathbf{u}}_1(d)\}$.

$\tilde{\mathbf{u}}_1(a)$	$\tilde{\mathbf{u}}_1(b)$	$\tilde{\mathbf{u}}_1(c)$	$\tilde{\mathbf{u}}_1(d)$
0.000	−0.348	−0.348	0.696
0.000	−0.500	−0.500	1.0
0.000	−0.3705	−0.3705	0.741
0.000	−0.258	−0.258	0.516
0.000	−0.258	−0.258	0.516
0.000	−0.258	−0.258	0.516

corresponding to this mode in the cluster labeled d. However, $\sum_{i=1}^{3}\mathbf{u}_2(i)=0$ indicates that there are only two independent eigenvectors corresponding to this mode in the cluster under consideration. Finally, since there are four equivalent clusters (as dictated by the local symmetry), which are now decoupled, the mode thus becomes an eightfold degenerate mode.

In conclusion, we have demonstrated the unique feature of the real space Green's function in the calculation of the eigenvectors of degenerate states by studying the persistent degenerate mode exhibited by the Vicsek fractal. In particular, we found that the lowest persistent degenerate mode of the third-stage Vicsek fractal is an edge-confined, superlocalized mode. The persistence and the evolution of the degenerate mode are shown to be the consequence of the interplay between the local geometry and the self-similar nature of the fractal. For our model fractal, the persistence of a vibrational mode is found to arise due to the decoupling of the four equivalent branches, which in turn is due to the zero displacement vector field associated with the central cluster. Finally, because of the common feature shared by the Vicsek fractal and the fractal drum investigated by Sapoval, Gobron, and Margolina (four equivalent regions coupled through a central region), we feel that the observed confinement of the low-lying vibrational mode on the fractal drum may be understood using the same physical reasoning.

We acknowledge the support of the NSF (EHR-9108764) and the Research Corporation grants.

[1] W. Press, B. P. Flannery, S. A. Teukolsky, and W. T. Vettering, *Numerical Recipes* (Cambridge Univ. Press, Cambridge, 1989).

[2] B. Sapoval, Th. Gobron, and A. Margolina, Phys. Rev. Lett. **67**, 2974 (1991).

[3] J. E. Black, Phys. Rev. B **38**, 2151 (1988).

[4] R. Rammal, J. Phys. (Paris) **45**, 191 (1984); S. H. Liu, in *Solid State Physics*, edited by H. Ehrenreich, F. Seitz, and D. Turnbull (Academic, New York, 1986), Vol. 39, p. 207.

[5] S. Y. Wu, in *Progress in Statistical Mechanics*, edited by C. K. Hu (World Scientific, Singapore, 1988), p. 119.

[6] C. Kittel, *Introduction to Solid State Physics* (Wiley, New York, 1976), p. 122.

[7] C. S. Jayanthi and S. Y. Wu (to be published).